Int. J. Electrochem. Sci., 11 **(2016)** 1530 - 1540

International Journal of ELECTROCHEMICAL SCIENCE
www.electrochemsci.org

Electrocatalytic Oxidation Behavior of Cefixime Antibiotic at Bimetallic Pt-W Nanoparticle-Decorated Multi-Walled Carbon Nanotubes Modified Glassy Carbon Electrode and its Determination

Ali Fakhri[1,*], *Sara Shahidi*[2], *Shilpi Agarwal*[3,4], *Vinod Kumar Gupta*[3,4,*]

[1]Young Researchers and Elites Club, Science and Research Branch, Islamic Azad University, Tehran, Iran
[2]Department of Materials Engineering, Central Tehran Branch, Islamic Azad University, Tehran, Iran
[3]Department of Chemistry, Indian Institute of Technology Roorkee, 247667, India
[4]Department of Applied Chemistry, University of Johannesburg, Johannesburg, South Africa
[*]E-mail: ali.fakhri88@yahoo.com, vinodfcy@iitr.ac.in, vinodfcy@gmail.com

Received: 12 October 2015 / *Accepted:* 2 November 2015 / *Published:* 1 January 2016

In this project, we presented a new method for synthesis of multi-walled carbon nanotube-supported platinum–tungsten alloy nanoparticles (Pt-W/MWCNTs) by facile one-step alcohol-reduction process. The synthesized Pt-W/MWCNTs composites were characterized using X-ray diffraction (XRD), transmission electronic microscopy (TEM) and Field-emission scanning electron microscope (FE-SEM). To consider the catalytic efficiency of Pt-W/MWCNTs composites, the electro-oxidation of cefixime antibiotic using the Pt-W/MWCNTs composites on glassy carbon electrode (Pt-W/MWCNTs/GCE) was tested in buffer solution (pH 7.0) using linear sweep voltammetry (LSV) and cyclic voltammetry (CV). Bare GCE demonstrates a passive oxidation wave around 1.02 V for cefixime antibiotic whereas Pt-W/MWCNTs/GCE demonstrates an apparent oxidation peak at 0.66 V. The modified electrode does not indicate any fouling effect toward the oxidation of cefixime antibiotic. To describe the electrode modifying process, electrochemical impedance spectroscopy (EIS) was used. The amperometry method was applied to distinguish cefixime antibiotic in the concentration range of $1.0\text{x}10^{-8}$ to $3.2\text{x}10^{-6}$M with a detection limit of $5\text{x}10^{-9}$ M.

Keywords: Alloy nanoparticles, Carbon nanotubes, cefixime antibiotic, Electrocatalysis, Voltammetry

1. INTRODUCTION

Carbon nanotube (CNT) properties such as chemical stability, thermal conductivity, and high specific surface area, present them very attractive cases for use as nano templates for the stabilization and dispersion of metal nanoparticles [1]. A novel class of materials like metal nanoparticles (NPs) shows unparalleled physical properties and they clearly varied from those of the bulk [2,3]. NPs offers many major applications such as magnetism, catalysis [4], biomedicine [5] and cancer therapy [6].

Nowadays, the abuse from antibiotics has drawn special attention. According to some earlier reports, great antibiotics are pharmaceutical remnants and endocrine disruptors which have been discarded altogether into the environment. Cefixime is an antibiotic beneficial for the treatment of a number of bacterial infections. It is a third generation cephalosporin.

Electrochemical sensors based on nanoparticles have gained major attention recently due to their high surface area, good stability and unique electrochemical properties [7,8]. It is broadly employed for metal nanomaterials [9], graphene [10,11], carbon nanotube [12,13] and so on. Many earliest reports show that platinum nanomaterials could be applied as catalysts for oxidation reactions [14,15]. The stability and sensitivity of electrochemical sensors have been improved severely by the use of the Pt nanoparticles [16,17].

Bimetallic nanoparticle catalysts usually include a primary and secondary metals, and those play an important role in catalytic activity. Primary metal has a high efficiency in catalytic activity and a secondary metal can be used to affect the catalytic activity or impede poisoning difficulties [18,19]. Due to their selectivity, stability and activity compared to the separate components, bimetallic nanoparticles is used as a synergetic catalyst in the electrochemical reactions [20–29].

In this work, we investigated synthesis and catalytic activity of Pt-W/MWCNTs composites system. The Pt-W alloy nanoparticles and multi-walled carbon nanotubes composite modified glassy carbon electrode was examined for the electrochemical oxidation of cefixime antibiotic using cyclic voltammetry. The proposed modified electrode shows good response towards cefixime and it was successfully applied for determination of cefixime antibiotic.

2. EXPERIMENTAL

2.1. Reagents and Apparatus

Catalytic chemical vapor deposition (CVD, purity > 95%) with tube length of 0.5–200 nm and inner diameter of 5–10 nm and outer diameter of 10–20 nm was obtained from Nanostructured & Amorphous Materials (Houston, TX, USA). Cefixime (99%) was obtained from Hangzhou Dayangchem Co. (Hangzhou, China) and used as received. All the other chemicals were obtained from Sigma-Aldrich Ltd, USA. All the chemicals used for the study were of analytical grade.

Field-emission scanning electron microscope (FE-SEM, JEOL 2010 F), transmission electron microscopy (TEM, JEM- 2100F HR, 200 kV), and X-ray diffractometer (XRD) Philips X’Pert were used to characterize the adsorbent for its morphological information. All the electrochemical experiments were performed with a conventional three–electrode electrochemical cell using a μAUTOLAB Type III Potentiostate-Galvanostate with computerized control by GPES (General Purpose Electrochemical Software) soft-ware at room temperature. A platinum wire was used as the auxiliary electrode, glassy carbon electrode (3 mm diameter) as working electrode and a double junction Ag/AgCl/KCl (saturated) electrode was employed as the reference electrode.

2.2. Preparation of multi-walled carbon nanotube-supported platinum–tungsten alloy nanoparticles (Pt-W/MWCNTs)

Before use, the purchased MWCNTs were acid-treated by refluxing in a mixture of concentrated H_2SO_4 and HNO_3 (v/v, 3:1) for 8 h at 80°C. The Pt-W/MWCNTs composites were prepared by a facile one-step alcohol-reduction process. In brief, 10 mg MWCNTs were dispersed into the solution of 20 mL ethylene glycol and 20 mL deionized water. Then, 300 mg trisodium citrate, 50 μmol H_2PtCl_6 and 50 μmol $Na_2WO_4{\cdot}2H_2O$ were added to the mixture above. After sonication for 30 min, the pH of the misture was adjusted to 10 with NaOH. A solution of sodium borohydride ($NaBH_4$) was further added to the suspension under vigorous stirring followed by sonication for 30 min. The mixture solution was deoxygenated by nitrogen for 30min and reacted for 8 h. Finally, the composites was washed with water and dried for characterization and measurement.

2.3. Fabrication of Pt-W/MWCNTs/GCE

Suspensions of 0.5 mg mL^{-1} Pt-W/MWCNTs composites, were prepared by mixing the appropriate amount of the catalysts in THF. After sonication for 10 min, suspensions were vigorously stirred for 48 h before use. Prior to the modification, GC electrodes were polished with aluminum oxide (0.01 mm), rinsed thoroughly with double distilled water, sonicated for 1 min in double distilled water, rinsed with double distilled water and dried under oven. Modification of the GC electrodes was achieved by dropping 10 mL of Pt-W/MWCNTs composites suspensions over the active surface and left the solvent to evaporate overnight.

3. RESULTS AND DISCUSSION

3.1. Characterization of the Pt-W/MWCNTs hybrid

Fig. 1 indicates the XRD Spectra of MWCNTs and Pt-W/MWCNTs composites. The diffraction peak at ca. 2θ=26.1° is corresponded to the graphite structure (002) plane in MWCNTs sample. Fig. 1B provided the XRD patterns of Pt-W/MWCNTs composite could be indexed as platinum on MWCNTs, with all peaks corresponding well to standard crystallographic data (shown the diffraction peaks of Pt (111), (200), (220) and (311) planes of face-centered cubic crystalline platinum). No other impurities were determined, which indicates the high-purity products. Our computation from the XRD patterns according to Scherrer equation (eq. 1) demonstrates the average particles sizes of Pt-W/MWCNTs composite is 5.1 nm.

$$D = \frac{K\lambda}{\;} \qquad (1)$$

where K = 0.94 is the shape factor, β is the full width at half maximum given in radians, λ is a wavelength of X-ray, and θ is the angle between the incident ray and the scattering planes [30,31].

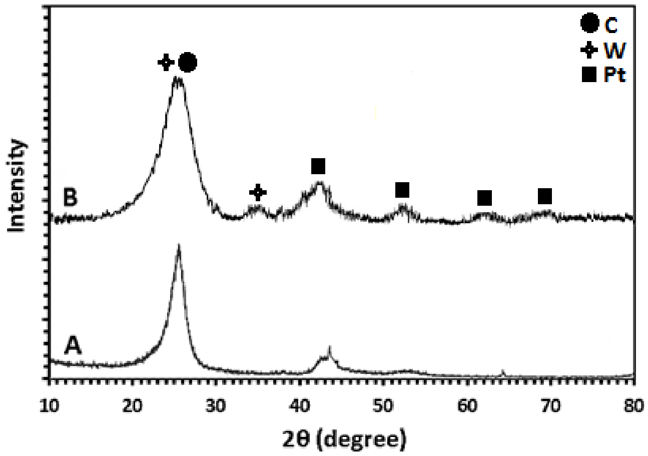

Figure 1. XRD patterns of (A) MWCNTs, (B) Pt-W/MWCNTs composite.

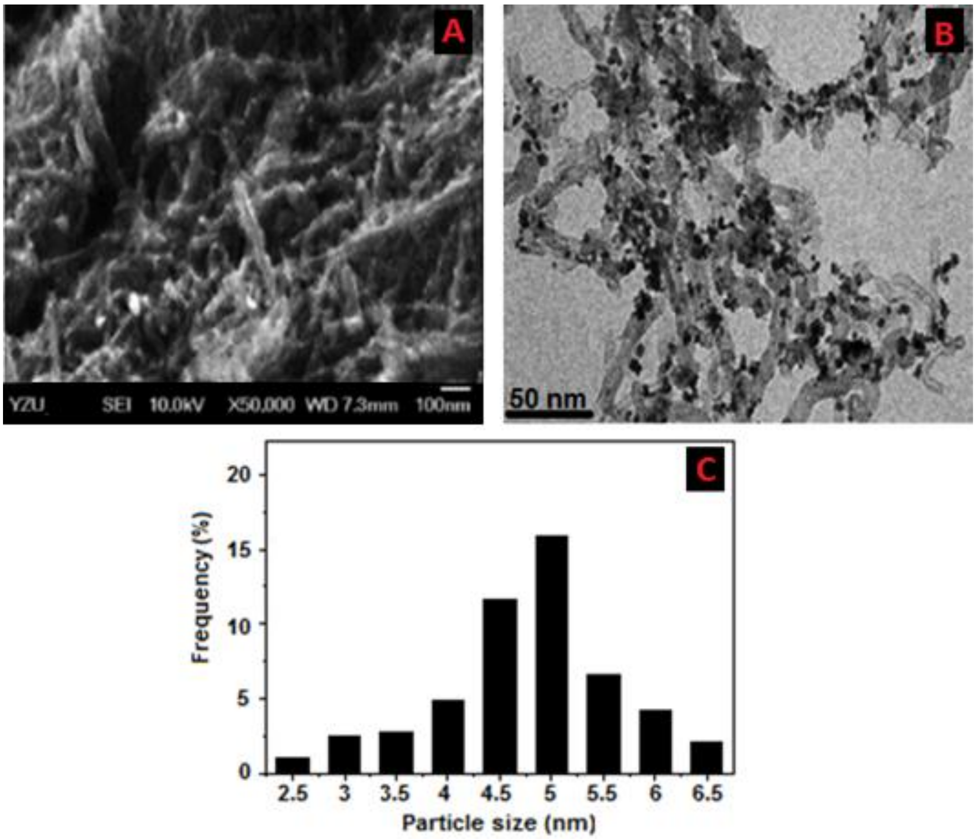

Figure 2. FE-SEM image (A), TEM image (B) and histogram of the diameter distribution (C) of Pt-W/MWCNTs composite.

The particle distribution and morphology of Pt-W alloy on MWCNTs, and the agglomeration status of particles of Pt-W alloys can be obviously observed in the SEM images. From the FE-SEM images of Fig. 2(A), as is evident, that the MWCNTs and the Pt-W particles were tangled together to form agglomerated particles.

Fig. 2(B) indicates the morphology of the as-prepared composites. It is found that Pt-W nanoparticles are uniformly deposited on the surface of MWCNTs without clear aggregation. The size distribution is investigated statistically by measuring the diameter of Pt-W nanoparticles in the selected area (Fig. 2(C)). The Pt-W nanoparticles have a mean size of 5.0 nm, with an arrow size distribution.

3.2. Electrochemical behavior of Pt-W/MWCNTs/GCE

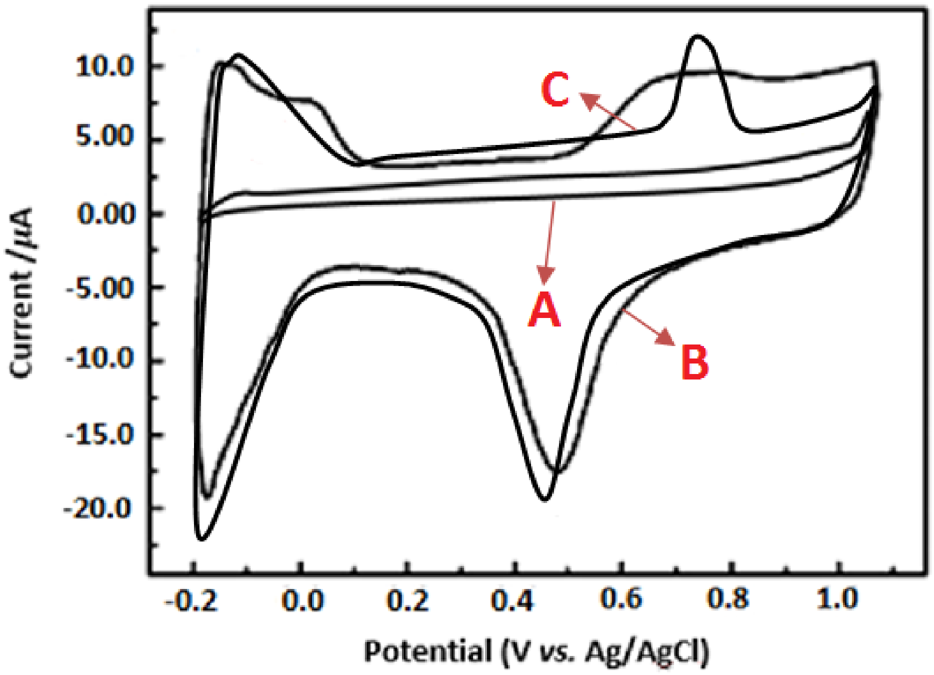

Figure 3. Cyclic voltammograms of unmodified GCE (A), and to Pt-W/MWCNTs/GCE (B) at a scan rate of 50 mV s^{-1} in 0.5 M H2SO4 at 25°C and to Pt-W/MWCNTs/GCE (C) in cefixime antibiotic (1×10^{-5} M) with 0.5 M H_2SO_4 at a scan rate of 50 mV s^{-1}.

The cycle voltammograms of bare GCE and Pt-W/MWCNTs/GCE in 0.5 M sulfuric acid at 50 mVs^{-1} are indicated in Fig. 3. The CV scans start from an open circuit potential and then sweep within the potential region between −0.2 V and 1.0 V vs. Ag/AgCl. All catalyst electrodes display a resemble configuration within the potential region. There are three regions exhibiting in the CV feature: The peak (1) adsorption/desorption of H atoms onto catalyst (−0.2–0.2V); the peak (2) Corresponding to the process of oxidation reactions, emerging at 0.47 V, can be attributed to the reduction of the platinum oxide during the negative sweep; and the peak (3) emerges about between 0.55 to 1.0 V can be due to the generation of the platinum oxide layer on the catalyst surface.

Herein the ESA value of catalysts can thus be determined from

$$ESA = \frac{Q_H}{0.21} \qquad (2)$$

where Q_H is the specific charge transfer contributed from catalysts (in units of C g^{-1}), and the factor 0.21 (in units of mC cm^{-2}) is distinguished from electrical charge associated with monolayer adsorption of hydrogen on platinum [32].

It is totally recognized that the ESA value serves as a crucial factor in determining the number of active sites for electrochemically adsorbing/desorbing H atoms onto the catalyst surface. After the computation, the ESA value is 38.15 (m^2 g^{-1}).

3.3. Electrochemical determination of cefixime antibiotic at Pt-W/MWCNTs/GCE

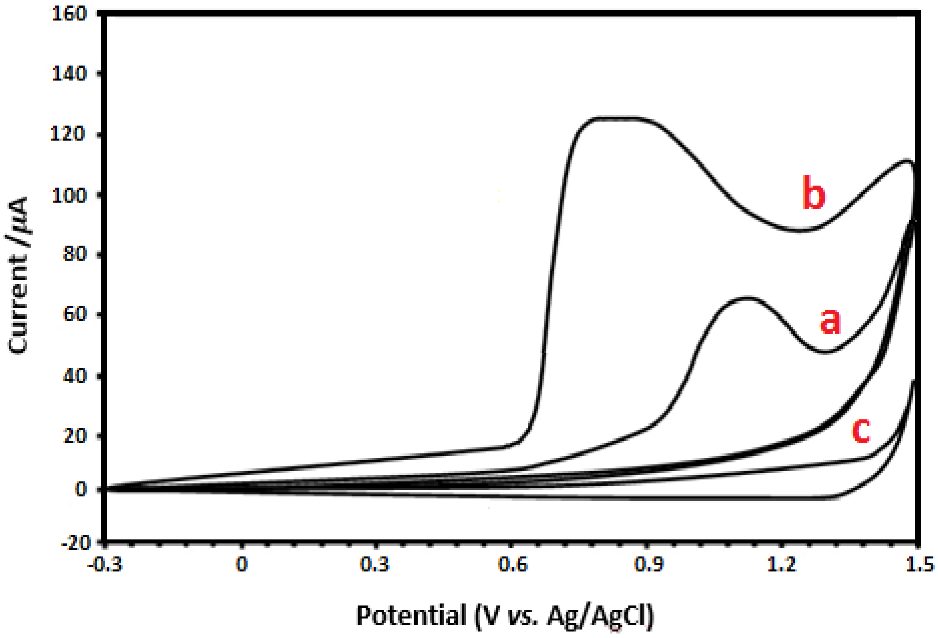

Figure 4. Cyclic voltammograms of cefixime antibiotic (1 × 10^{-5} M) in phosphate buffer solutions (pH 7.00) using (a) GCE, (b) Pt-W/MWCNTs/GCE and (c) blank sample using Pt-W/MWCNTs/GCE at a scan rate of 50 mV s^{-1}.

We have tested the electrocatalytic activity of Pt-W/MWCNTs deposited on GCE against cefixime antibiotic electro-oxidation in phosphate buffer solutions (pH 7.00) using cyclic voltammetry (Fig. 4). We obtained higher oxidation current with less positive potential for cefixime antibiotic at pH 7.00. Bare GCE shows an oxidation wave at 1.02 V for cefixime antibiotic (curve a). On the other hand, the Pt-W/MWCNTs modified GCE exhibits an apparent oxidation wave for cefixime antibiotic at 0.66 (curve b). A comparison of the cyclic voltammograms of cefixime antibiotic at bare GCE (curve a) and Pt-W/MWCNTs/GCE (curve b) indicates the oxidation peak potential of cefixime antibiotic at Pt-W/MWCNTs/GCE occurs at a potential about 360 mV less positive than at a bare GCE. The founded obvious voltammetric signal with less positive potential and higher oxidation current for cefixime antibiotic at Pt-W/MWCNTs/GC electrode was attributed that the oxidation of cefixime antibiotic was catalyzed by Pt-W/MWCNTs/GCE.

3.4. Effect of pH on cefixime antibiotic oxidation

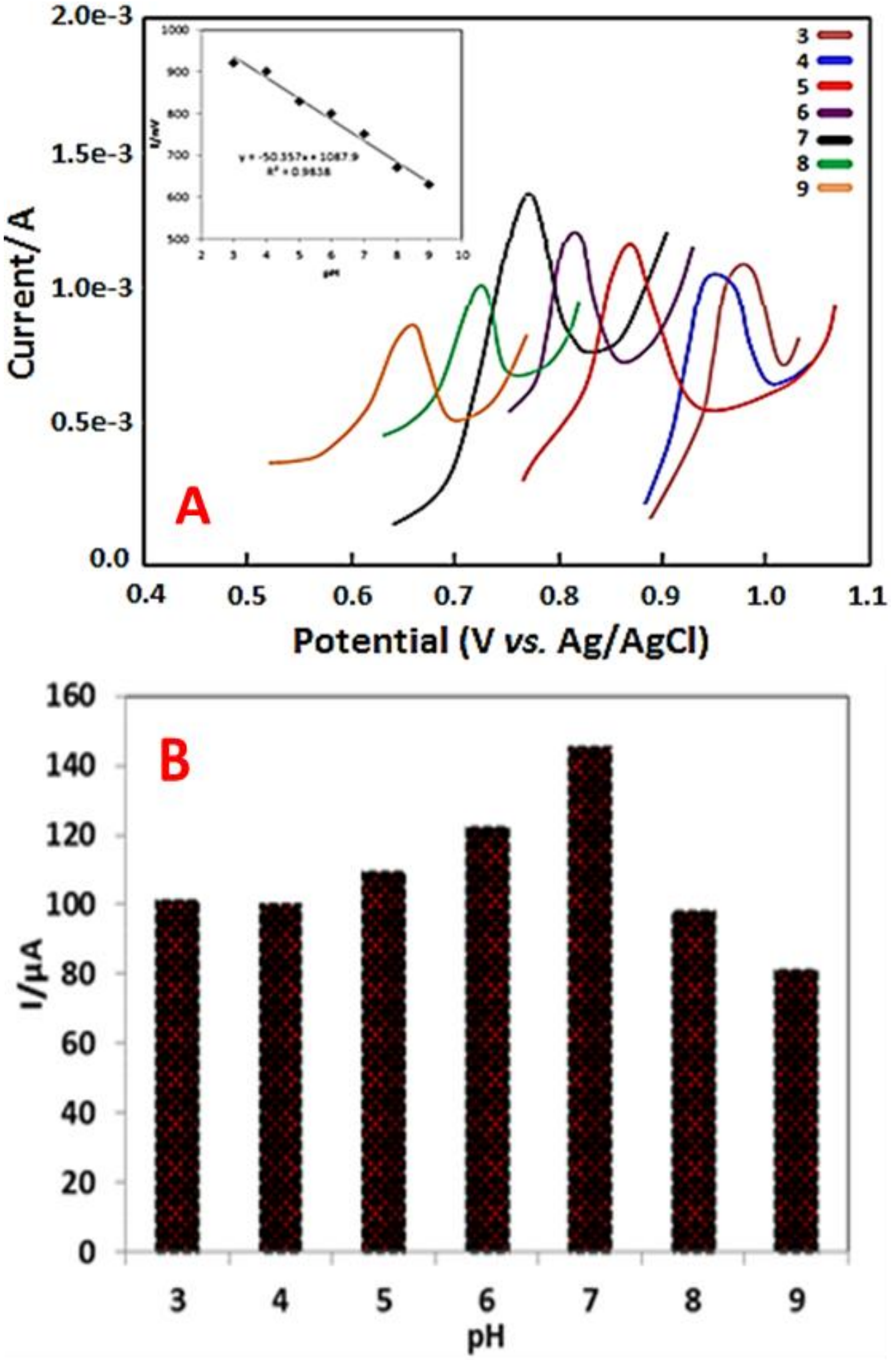

Figure 5. (A) LSVs for 1 μmol L^{-1} cefixime at Pt-W/MWCNTs/GCE in various pHs (from 3.0 to 9.0) of buffer solution (The inset is dependence the oxidation peak potential with pH solution, (B) the diagram of pH value influence on the oxidation peak current; Supporting electrolyte was BR buffer solution and sweep rate was 50 mV s^{-1}.

The electrochemical behavior of cefixime antibiotic are dependent on the pH value of solution [33,34]. To evaluate the optimum pH for cefixime detection on the surface of the modified electrode, its electrochemical behavior was investigated in the buffered solutions with various pHs in the range of 3–9 (Fig. 5). A linear negative shift was observed in the anodic peak potential of cefixime by increasing pH according to Eq. (3):

$$y = -50.557x + 1047.9 \qquad (3)$$

Observation of a slope of −50 mV per pH unit confirms the contribution of an equal number of protons and electrons in the electrochemical reaction of cefixime. Based on such investigations, a buffered solution of pH 7.0 was chosen as an optimum condition in order to obtain the best sensitivity in all voltammetric measurements.

3.5. Amperometric determination of cefixime antibiotic

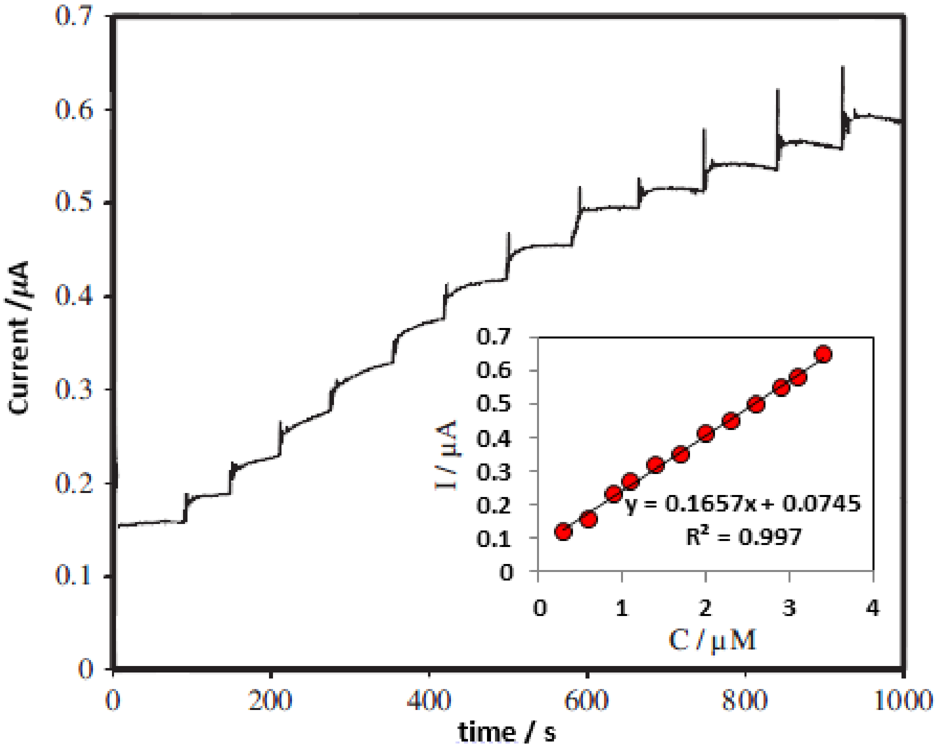

Figure 6. Current–time curve of Pt-W/MWCNTs/GCE with successive addition of cefixime antibiotic to a stirred 0.1 M PBS (pH 7.00); the inset is the calibration curve.

To improve the sensing efficiency of the electrode, the effect of the applied potential on the response of the sensor was tested. Current–time curves were recorded at different applied potential in successive addition a certain amount of cefixime antibiotic (not shown). The results showed that the corresponding maximum respond was observed at the applied potential 0.6 V. Fig. 6 indicates the typical steady-state current–time response of the Pt-W/MWCNTs/GCE in 0.1 M PBS with consecutive injection a certain amount of cefixime antibiotic at +0.6 V. The response time was within 5s, suggesting a facile electron-transfer process through the Pt-W/MWCNTs. The Pt-W/MWCNTs/GCE demonstrated an apparent concentration dependence. The relationship between the electro-catalytic current and cefixime antibiotic in different concentration at the Pt-W/MWCNTs/GCE is shown in the inset of Fig. 6, demonstrating a good linear relationship in the range of $1.0x10^{-8}$ to $3.2x10^{-6}$ M (correlation coefficient = 0.996). The detection limit of cefixime antibiotic at the electrode is $5x10^{-9}$ M (S/N=3). The sensitivity of the present cefixime sensor is 1.6051 $\mu A \mu M^{-1}$.

A comparison of the applicability and analytical part of the present sensor with some of the previous reports on the cefixime determination in terms of their working electrode, technique, detection limit and linear range was given in Table 1.

Table 1. Analytical parameters for detection cefixime antibiotic at several modified electrodes.

Technique	Type of electrode	LOD (μM)	Linear range (μM)	Ref.
DPP	HMDE	0.046	0.06–12.0	[22]
SWV	HMDE	0.064	6.0–200.0	[23]
SWV	HMDE	0.008	0.056–0.110	[24]
SWV	GNPs/MWCPE	0.003	0.01–200	[25]
CV	$NiFe_2O_4$-MWCNTs/GCE	0.09	0.1–600	[29]
Amperometry	Pt-W/MWCNTs/GCE	0.005	0.01-3.2	This study

3.6. Reproducibility and stability of the Pt-W/MWCNTs/GCE

The operational stability of Pt-W/MWCNTs/GCE was tested by the CV method every 2 days in 2 weeks. The response to 0.1 mM cefixime antibiotic reduced less than 12% after 2 weeks, so it has excellent stability. The construction reproducibility of five electrodes independently made, indicated a RSD of 3.1% for detecting 0.1 mM cefixime antibiotic. The good reproducibility and stability of Pt-W/MWCNTs/GCE may be mainly attributed to the strong deposition of the Pt-W/MWCNTs.

The effect of some inorganic ions and some biomolecules on the electrochemical oxidation of 10 μM cefixime has been evaluated. It was found that 50-fold concentration of glucose and ascorbic acid (AA), 100-fold concentration of Cu^{2+}, Na^{+}, K^{+}, NO_3^{-}, Cl^{-}, Li^{+} and SO_4^{2-}did not interfere with the cefixime tests (signal change below 1.45%).

3.7. Reproducibility and stability of the Pt-W/MWCNTs/GCE

Electrochemical impedance spectroscopy (EIS) was also used to study the characteristics of the modified electrode. In the EIS, The semicircle diameter of Nyquist plot corresponds to the electron transfer limited process and the diameter is equivalent to the electron transfer resistance (R_{ct}). Fig. 7 shows the results of EIS on a bare GC electrode (a) and Pt-W/MWCNTs/GC electrode (b) in an electrolyte of 0.1 mol L^{-1} KCl and equimolar of $[Fe(CN)_6]^{4-/3-}$. As seen, almost linear EIS was observed for bare GC electrode (curve a), showing a very low electron transfer resistance to the redox probe. However, the R_{ct} increased on the Pt-W/MWCNTs/GC electrode (curve b), confirming the formation of membrane layer on the electrode surface, which exhibited a barrier effect to the electron transfer kinetics. The impedance change of the modification process suggests that nano-Pt-W/MWCNTs are indeed electrically contacted with the glassy carbon electrode surface.

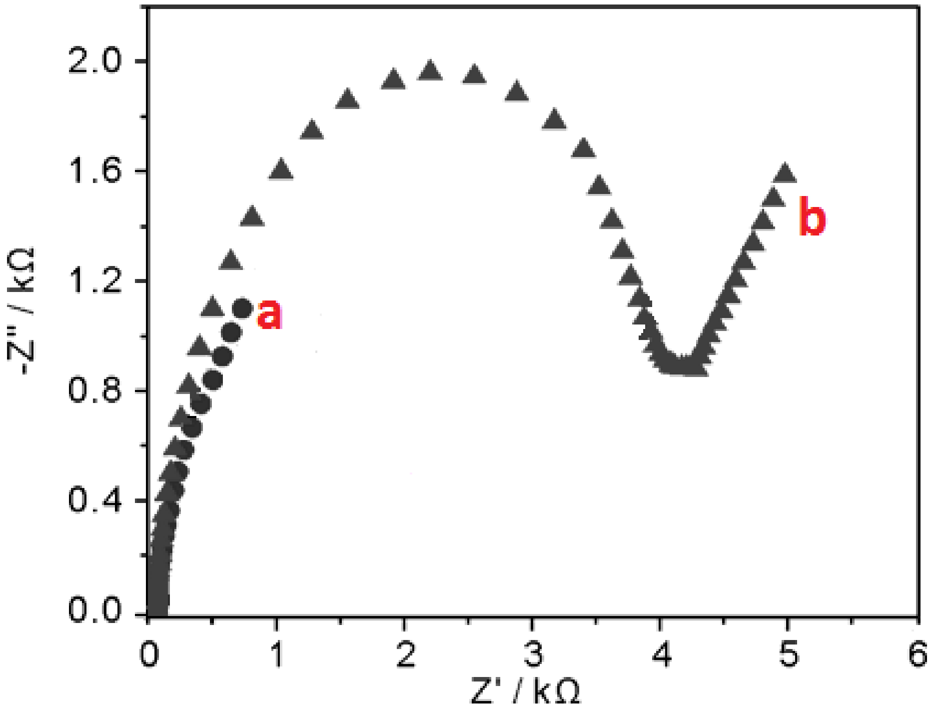

Figure 7. Nyquist diagram of electrochemical impedance spectra of (a) bare glassy carbon electrode; (b) Pt-W/MWCNTs/GC electrode in 0.1 mol L^{-1} KCl and equimolar of $[Fe(CN)_6]^{4-/3-}$.

4. CONCLUSIONS

The present study indicated that Pt-W/MWCNTs composite can be readily formed by facile one-step alcohol-reduction process. The Pt-W/MWCNTs composite has catalytic activity, making it an ideal case for sensor utilizations. This study shows the sensitive determination of cefixime antibiotic using the Pt-W/MWCNTs composite modified GCE. The bare GCE indicated a passive oxidation wave for cefixime antibiotic whereas the modified electrode not only demonstrated an apparent stable oxidation peak but so enhanced its oxidation current. In addition, using the amperometry method, a detection limit of 5×10^{-9} M (S/N = 3) was achieved for distinguished of cefixime antibiotic. The modified electrode indicated good reproducibility and stability.

ACKNOWLEDGEMENT
The author acknowledges Materials & Energy Research Center and Razi Metallurgical Research Center (RMRC) from Iran for performance support through the project.

References

1. G. G. Wildgoose, C. E. Banks and R. G. Compton, *Small*, 2 (2006) 182.
2. C. N. R. Rao, G. U. Kulkarni, P. J. Thomas and P. E. Peter, *Chem. Eur. J.*, 8 (2002) 28.
3. G. Hodes, *Adv. Mater.*, 19 (2007) 639.
4. S. J. Liu, C. H. Huang, C. K. Huang and W. S. Hwang, *Chem. Commun.*, 32 (2009) 4809.
5. A. K. Gupta and M. Gupta, *Biomater.*, 26 (2005) 3995.

6. H. Hong, Y. Zhang, J. Sun and W. Cai, *Nano Today*, 4 (2009) 399.
7. A. Chattopadhyay, M. P. Sk and C. K. Jana, *Chem. Commun.*, 49 (2013) 8235.
8. X. Luo, A. Morrin, A. J. Killard and M. R. Smyth, *Electroanal.*, 18 (2006) 319.
9. X. Chen, H. Pan, H. Liu and M. Du, *Electrochim. Acta*, 56 (2010) 636.
10. B. J. Sanghavi, S. Sitaula, M. H. Griep, S. P. Karna, M. F. Ali and N. S. Swami, *Anal. Chem.*, 85 (2013) 8158.
11. B. J. Sanghavi, W. Varhue, J. L. Chávez, C. -F. Chou and N. S. Swami, *Anal. Chem.*, 86 (2014) 4120.
12. J. Wang, *Analyst*, 130 (2005) 421.
13. B. J. Sanghavi and A. K. Srivastava, *Electrochim. Acta*, 55 (2010) 8638.
14. X. Zhu, X. Niu, H. Zhao, J. Tang and M. Lan, *Biosens. Bioelectron.*, 67 (2015) 79.
15. C. T. Hsieh, Y. S. Chang, A. K. Roy, P. Y. Yu, K. M. Yin, *Electrochim. Acta*, 149 (2014) 278.
16. H. Duan and C. Xu, *Electrochim. Acta*, 152 (2015) 417.
17. L. Elbaz, C. R. Kreller, N. J. Henson and E. L. Brosha, *J. Electroanal. Chem.*, 720-721 (2014) 34.
18. C. H. Yen, K. Shimizu, Y. Lin, F. Bailey, I. F. Cheng and C. M. Wai, *Energy Fuels*, 21 (2007) 2268.
19. J. R. Croy, S. Mostafa, L. Hickman, H. Heinrich and B. R. Cuenya, *Appl. Catal. A Gen.*, 350 (2008) 207.
20. N. Toshima and T. Yonezawa, *New J. Chem.*, 22 (1998) 1179.
21. R. Ferrando, J. Jellinek and R. L. Johnston, *Chem. Rev.*, 108 (2008) 845.
22. T. M. Reddy, M. Sreedhar and S. J. Reddy, *J. Pharm. Biomed. Anal.*, 31 (2003) 811.
23. A. Golcu, B. Dogan and S. A. Ozkan, *Talanta*, 67(2005) 703.
24. R. Jain, V. K. Gupta, N. Jadon and K. Radhapyari, *Anal. Biochem.*, 407 (2010) 79.
25. A. Afkhami, F. S. Felehgari and T. Madrakian, *Electrochim. Acta*, 103 (2013) 125.
26. D. P. Santos, M. F. Bergamini and M. V. B. Zanoni, *Sens. Actuators B*, 133 (2008) 398.
27. S. Majdi, A. Jabbari, H. Heli, H. Yadegari, A. A. Moosavi-Movahedi and S. Haghgoo, *J. Solid State Electrochem.*, 13 (2009) 407.
28. S. Shahrokhian, N. Hosseini-Nassab and Z. Kamalzadeh, *J. Solid State Electrochem.*, 18 (2014) 77.
29. A. A. Ensafi and A. R. Allafchian, *Colloids Surf. B*, 102 (2013) 687.
30. B. Andonovic, M. Temkov, A. Ademi, A. Petrovski, A. Grozdanov, P. Paunovic and A. Dimitrov, *J. Chem. Technol. Metall.*, 49 (2014) 545.
31. L. Alexander and H. P. Klug, *J. Appl. Phys.*, 21 (1950) 137.
32. N. Y. Sreedhar, M. Sunil Kumar and K. Krishnaveni, *Sens. Actuators B*, 210 (2015) 475.
33. L. Agu, J. Manso, P. Yanez-Sedeno and J. M. Pingarron, *Talanta*, 64 (2004) 1041.
34. J. A. Cox and E. D. Zlotorzynska, *Electroanal.*, 3 (1991) 239.